Surface reconstruction and energy gap of superconducting V$_3$Si(001)

N. Hauptmann,[*] M. Becker, J. Kröger, and R. Berndt

Institut für Experimentelle und Angewandte Physik,
Christian-Albrechts-Universität zu Kiel, D-24098 Kiel, Germany
(Dated: March 19, 2009)

A yet unknown surface reconstruction of V$_3$Si(001), which is most likely induced by carbon, is used to investigate the quasi-particle energy gap at the atomic scale by a cryogenic scanning tunneling microscope. The width of the gap was virtually not altered at and close to carbon impurities, nor did it change at different sites of the reconstructed surface lattice. A remarkable modification of the spectroscopic signature of the gap was induced, however, upon moving the tip of the microscope into controlled contact with the superconductor. Spectroscopy of the resulting normal-metal – superconductor junction indicated the presence of Andreev reflections.

PACS numbers: 68.35.bd, 68.37.Ef, 74.70.Ad, 74.45.+c

I. INTRODUCTION

Superconductivity is one of the most vividly investigated research fields in solid state physics. In particular, spectroscopy of the energy gap of the quasi-particle density of states (DOS) has attracted considerable interest. Modifications of the energy gap by local impurities or by passing high currents through superconducting junctions have been recently studied.[1,2,3,4,5,6,7,8,9,10,11,12,13,14,15] Effects of impurities on the energy gap[1,2,3,4,5,6,7,8,9,10] provided valuable information about the interplay between superconductivity and magnetism or about the Cooper-pairing mechanism in unconventional superconductors, while high currents through superconducting contacts were used to unravel the number and transmission probability of transport channels via the occurrence of Andreev reflections.[11,12,13,14,15] Until now such experiments have been restricted to conventional elemental superconductors with critical temperatures $T_c < 10\,\mathrm{K}$ or to unconventional cuprate-based superconductors.[16]

In this article we present results of a combined scanning tunneling microscopy (STM) and spectroscopy (STS) study of the superconducting compound V$_3$Si(001), which exhibits a yet unknown surface reconstruction. Auger electron spectroscopy (AES) reveals that this reconstruction is most likely induced by the presence of carbon. This surface is an ideal system to study possible local variations of the quasi-particle energy gap since it provides, owing to the reconstruction, carbon impurities and a spatially inhomogeneous geometry. Apart from these favorable properties, STM investigations of this surface are extremely scarce. Except for two investigations of the magnetic flux lines[17] and Josephson tunneling[18] on unreconstructed V$_3$Si(001) using STM and STS, to our knowledge no additional STM and STS data are available for this surface. By combining a structural analysis using STM and an investigation of electronic properties with STS we found that the width of the energy gap is virtually independent of the position on the surface, while the symmetry of the gap is affected. We further investigated the current dependence on the tip-surface distance, from which we extracted the local

apparent barrier height and the transition from tunneling to contact. At contact, spectra of the quasi-particle energy gap exhibited pronounced modifications compared to spectra acquired in the tunneling regime. These modifications are discussed in terms of Andreev reflections.

We used V$_3$Si, which belongs to the class of A$_3$B binary intermetallic compounds or, shortly, A15 materials. V$_3$Si exhibits the β-tungsten structure[19] and is a type-II superconductor with a critical temperature T_c of $17\,\mathrm{K}$.[20,21] It has interesting electronic properties[22,23,24] such as a strong temperature dependence of the magnetic and electronic susceptibility and a large specific heat. Furthermore, V$_3$Si undergoes a structural cubic-to-tetragonal phase transition at a temperature of $21.3\,\mathrm{K}$, which exhibits characteristics of a thermo-elastic martensitic phase transition.[25] The concomitant change of lattice parameters is below the detection limit of STM.[26] We further notice that the occurrence of structural domain walls, which is attended by the martensitic transition is not related with the observed surface reconstruction, since the reconstruction is present already at room temperature.

The (001) surface of V$_3$Si has attracted particular attention because of the hexagonal-to-square transformation of its vortex lattice structure[17,27,28,29,30] and the occurrence of surface reconstructions.[31,32] The energy gap has been determined by a variety of spatially averaging techniques[33,34,35,36,37,38,39,40,41] yielding two distinct values of the zero-temperature energy gap Δ_0 either in the range from $1.32\,\mathrm{k_B}\,T_c$ to $2.7\,\mathrm{k_B}\,T_c$ or in the range from $0.5\,\mathrm{k_B}\,T_c$ to $0.95\,\mathrm{k_B}\,T_c$. The existence of these two distinct values of Δ_0 has so far been explained by BCS theory in terms of overlapping bands.[33,42,43] The first range of energy gaps is in good agreement with the value predicted by single-band s-wave BCS theory ($\Delta_0 = 1.76\,\mathrm{k_B}\,T_c$).[44]

II. EXPERIMENT

Measurements were performed with scanning tunneling microscopes operated in ultrahigh vacuum with a

base pressure of 10^{-9} Pa and optimized for low temperatures of (7.5 ± 0.3) K and for room temperature. Chemically etched tungsten tips were further prepared *in vacuo* by annealing and argon ion bombardment, while gold tips were cut at ambient conditions and used for the experiment without further treatment. The V$_3$Si(001) surface of a polished single crystal was prepared by argon ion bombardment with ion energies between 0.5 and 2 keV and subsequent annealing at temperatures between 1100 and 1200 K. Temperature readings from the pyrometer used in the experiments have an uncertainty margin of $\approx \pm 50$ K. All STM images were acquired in the constant-current mode with the voltage applied to the sample. STS measurements were performed in the constant-height mode. Spectra of the differential conductance $(\mathrm{d}I/\mathrm{d}V)$ were acquired by superimposing a sinusoidal voltage signal (root-mean-square amplitude 1 mV, frequency 7.6 kHz) onto the tunneling voltage and by measuring the current response with a lock-in amplifier. For AES a cylindrical mirror analyser was used.

III. RESULTS AND DISCUSSION

A. Characterization of reconstructed V$_3$Si(001)

Depending on the preparation parameters, (2×1) reconstructed or (1×1) unreconstructed surfaces of V$_3$Si(001) have been reported previously by Zajac *et al.*[31] They found by low-energy electron diffraction and AES that annealing of V$_3$Si(001) at temperatures exceeding 1070 K leads to a (2×1) reconstruction, while the (1×1) substrate surface is obtained for annealing temperatures lower than 1020 K. Figure 1(a) shows a room-temperature STM image of a V$_3$Si(001) surface obtained using the preparation procedure introduced in the experimental section. The reconstruction observed here does not match the previously observed (2×1) or (1×1) meshes.

Terraces which exhibit parallel lines are observed. The corrugation of these lines is (0.06 ± 0.02) nm and almost independent of the voltages applied in the experiments $(|V| \leq 1.5\,\mathrm{V})$. The distance between two adjacent lines is (1.8 ± 0.1) nm, which is approximately four times the lattice constant of V$_3$Si, $d = 0.47$ nm. The lines on adjacent terraces are either parallel [not shown in Fig. 1(a)] or orthogonal with respect to each other. The step height between adjacent terraces with orthogonal orientation of the lines is (0.23 ± 0.05) nm, which corresponds to half a lattice constant of V$_3$Si. Step heights between adjacent terraces with a parallel orientation of the lines are (0.47 ± 0.05) nm, which is similar to the V$_3$Si lattice constant. Based on these observations we can tentatively identify the origin of the lines. To this end we refer to the inset of Fig. 1(a), which depicts a model of the V$_3$Si lattice structure. Small filled spheres represent silicon atoms whereas large filled spheres represent vanadium atoms. The lattice constant d is identical with the spacing of
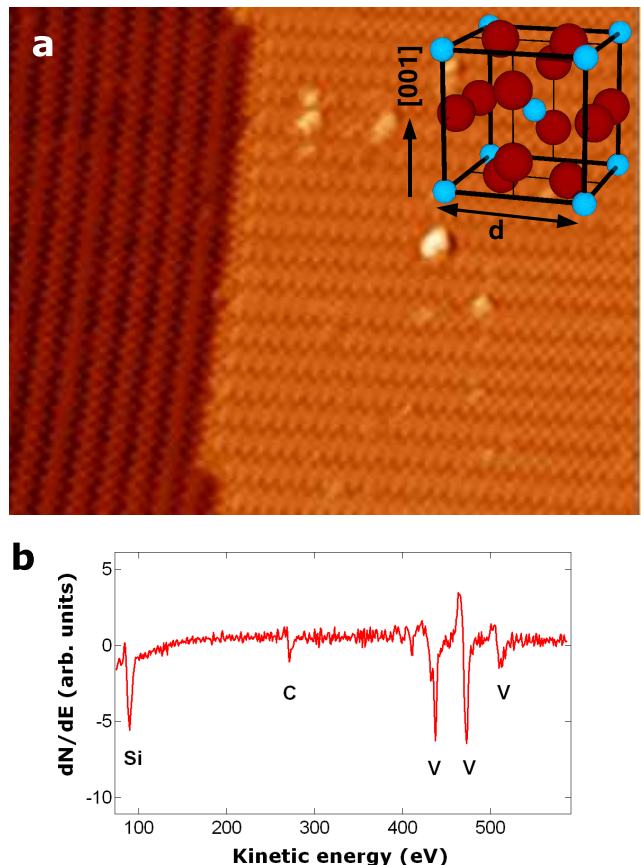

FIG. 1: (Color online) (a) STM image of two adjacent terraces on V$_3$Si(001) at room temperature (420 mV, 2.4 nA, 50 nm × 40 nm). The parallel lines visible on the terraces are due to a reconstruction of the surface, which is discussed in the text. Inset: β-tungsten lattice structure (Small filled spheres: silicon atoms, large filled spheres: vanadium atoms). The arrow indicates the [001] direction. (b) Auger spectrum of the reconstructed V$_3$Si(001) surface acquired with a kinetic energy of impinging electrons of 3 kV. Silicon (92 eV), carbon (274 eV), and vanadium (439 eV, 475 eV, 512 eV) peaks are identified according to Ref. 46.

the silicon sublattice. On an unreconstructed V$_3$Si(001) surface, vanadium atoms would form lines on the surface of a single crystal. According to this structural model, adjacent terraces with a step height of half a lattice constant exhibit lines of vanadium atoms, which are oriented perpendicular to each other. Analogously, terraces separated by one lattice constant show vanadium atom lines with the same orientation. This behavior matches our experimental observation and suggests that the lines originate from vanadium atoms. The mutual distance of the vanadium lines of $\approx 4d$, however, does not match the separation expected for the clean crystal.

To obtain more information about the reconstructed surface we used AES, which enables access to the chemical composition of the surface within the 5 top-most atomic layers depending on the material.[45] An Auger
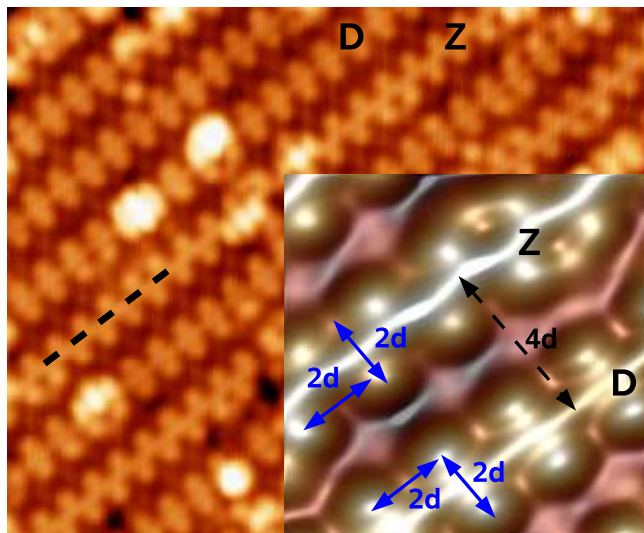
FIG. 2: (Color online) Atomically resolved STM image of a $V_3Si(001)$ terrace at $7.3\,K$ ($420\,mV$, $1\,nA$, $18\,nm \times 15\,nm$). Two characteristic lines, a dimer (D) and a zigzag (Z) line, appear on the terraces. Inset: Pseudo-three-dimensional presentation of close-up view ($4\,nm \times 4\,nm$) showing adjacent D and Z lines. The distance indicated by the solid arrows is $(0.9 \pm 0.1)\,nm \approx 2d$ where d denotes the lattice constant, while the lines are separated by $(1.8 \pm 0.1)\,nm \approx 4d$ (dashed arrow).

spectrum of the reconstructed V_3Si surface is shown in Fig. 1(b). In addition to spectroscopic signatures originating from vanadium ($439\,eV$, $475\,eV$, $512\,eV$) and silicon ($92\,eV$), a contribution from carbon ($274\,eV$) is observed. Following the quantitative analysis of Auger spectra exposed in Ref. 46, which takes into account the energy-dependent transmission function of the electron analyzer and the element-specific Auger sensitivity factors, the probed sample volume contains $\approx 8\,\%$ with respect to the total amount of detected elements. Taking into account the inelastic mean free path of carbon Auger electrons, we estimated that substrate layers within three to four lattice constants contribute significantly to the signal, so that the amount of carbon of $\approx 8\,\%$ gives the relative carbon concentration close to the surface. After excluding several other carbon sources such as the argon gas used for ion bombardment, the sample holder and the experimental setup, we surmise that carbon segregates from the bulk to the surface. Similar carbon-induced reconstruction like the one reported here have been reported for Si(001) and W(110). [47,48,49,50] In the latter case, carbon atoms arrange in a zigzag pattern, which is similar to our observations.

Figure 2 shows an STM image of a reconstructed surface area at $7.3\,K$ in more detail. Two types of lines can be observed. The first type of lines shows circular protrusions which are arranged in a zigzag (Z) pattern on both sides of the line (dashed line). The same protrusions occur on opposite sites of the second type of lines and form a dimer (D) arrangement. We ascribe these protrusions

to carbon atoms, which are arranged on opposite sites of the vanadium lines. The dimer and zigzag lines do not appear in an alternating pattern. We observed, however, that a carbon atom of a dimer line always faces a carbon atom of an adjacent line along a perpendicular direction with respect to the vanadium lines. This behavior may indicate an attractive interaction between the atoms. Some impurities are observed, which appear as bright protrusions. The inset of Fig. 2 shows a close-up view of a dimer and a zigzag line. The distance between two carbon atoms in a dimer line (solid arrows in the inset of Fig. 2) is $(0.9 \pm 0.1)\,nm$, which is approximately two times the lattice constant of V_3Si. The same distance is obtained for zigzag lines if the carbon atoms on one side of a zigzag line are shifted by d along this line. Thus, a zigzag line can be obtained by shifting the carbon atoms on one side of a dimer line by the lattice constant. The fact that two carbon atoms have a distance of roughly twice the lattice constant indicates that carbon atoms occupy every second lattice site of the silicon sublattice. Taking into account the martensitic transition of V_3Si, the question may arise whether structural domain walls may be the origin of the reconstruction. However, the same reconstruction was observed at room temperature [Fig. 1(a)] and we conclude that the martensitic transition is not related with the observed surface reconstruction.

STM images of the same reconstructed surface area at several different tunneling voltages are shown in Fig. 3. Tip changes in between the acquisition of the different images can be excluded since all images were taken successively within $3\,min$. Furthermore, sudden changes in the tunneling current, which may indicate tip changes, were not observed. The vanadium lines become pronounced at small voltages ($\pm 100\,mV$), which is indicated by dashed black lines, whereas they are hardly observed at high positive and negative voltages. This may indicate a one-dimensional state at low energies around the Fermi energy, which is located on the lines. Two findings lend support to this idea. First, a one-dimensional state is in agreement with an electronic model for the DOS of V_3Si. [51,52,53] This model assigns quasi-one-dimensional character to the vanadium d electrons, which gives rise to sharp peaks in the DOS close to the Fermi energy. First-principles calculations of the bulk band structure [54,55,56,57,58,59] also exhibit an extremely narrow peak in the DOS right below the Fermi energy, which is mainly due to vanadium d electrons. We note, however, that the calculations consider the bulk electronic structure, which may be modified at the surface. As a second indication favoring the presence of a one-dimensional state we mention the observation and calculation of a quasi-one-dimensional state on Fe(100) with segregated carbon. [60,61] Similar to our observations carbon atoms form zigzag chains on Fe(100) and laterally confine Fe $s-d$ states, which gives rise to formation of a Fe surface state band with one-dimensional character near the Fermi level.
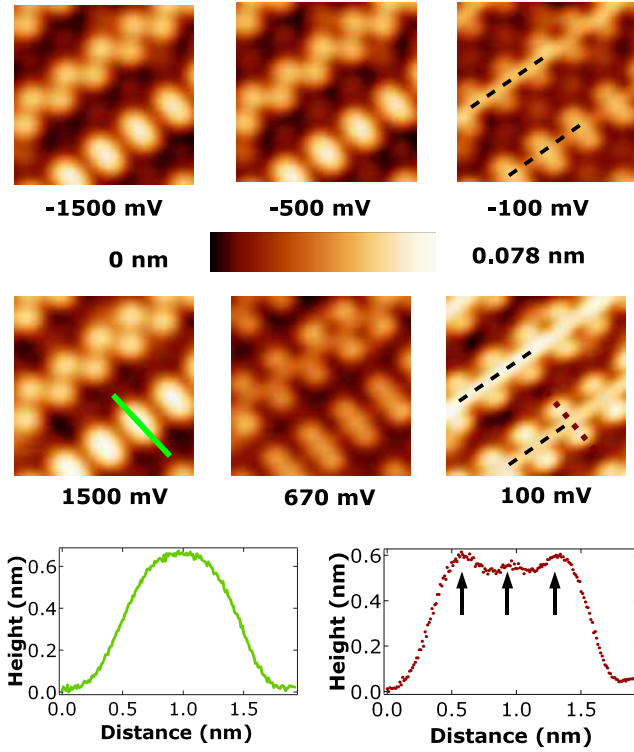
FIG. 3: (Color online) STM images of a reconstructed surface area ($1\,\mathrm{nA}$, $4\,\mathrm{nm} \times 4\,\mathrm{nm}$) taken at indicated voltages between -1500 mV and 1500 mV at 7.3 K. Two cross-sectional profiles of a dimer line are shown (positions are indicated by a solid and dotted line, respectively).
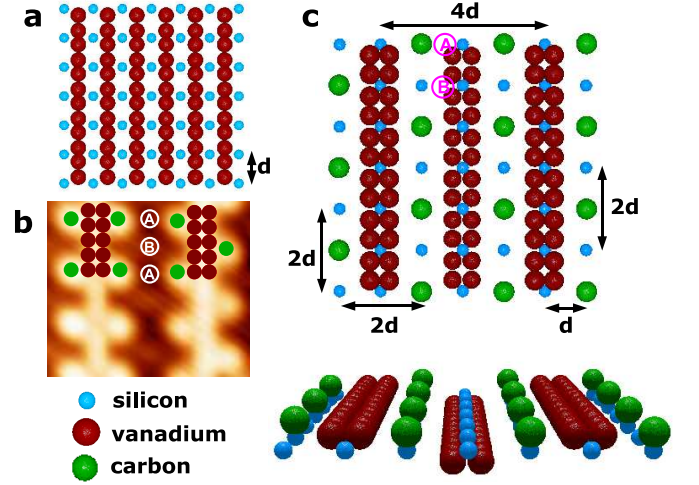

FIG. 4: (Color online) (a) Top-most surface layer of unre-constructed $V_3Si(001)$ surface (small filled spheres: silicon atoms, large filled spheres: vanadium atoms). (b) STM image ($100\,\mathrm{mV}$, $1\,\mathrm{nA}$) illustrating the model. Filled spheres denote carbon and vanadium atoms. (c) Top and side view of the top-most surface layer of the model of the reconstructed surface areas showing a dimer line and a zigzag line. A and B denote silicon atoms embedded in different environments regarding the neighbor atoms.

At small positive voltages ($100\,\mathrm{mV}$) the dimers in the dimer lines can clearly be distinguished as two atoms whereas at high negative and positive voltages ($\pm 1500\,\mathrm{mV}$) only a smeared shape can be seen. Two line scans on a dimer line are shown in Fig. 3, which were taken at positions indicated by the solid and dotted line, respectively. At $100\,\mathrm{mV}$ (right line scan in Fig. 3), the line and the two carbon atoms can be clearly distinguished (black arrows), while at $1500\,\mathrm{mV}$ (left line scan in Fig. 3), only a smeared shape can be seen. This loss of resolution can be understood on general grounds. Assuming a constant electronic structure of the STM tip, the tunneling current is an integral over the sample local density of states multiplied by a barrier transmission factor. The higher the tunneling voltage, the larger is the number of states contributing to the tunneling current. As a consequence, the localized one-dimensional state is dominated by other states. Only imaging at low voltages (here at $\pm 100\,\mathrm{mV}$) gives rise to the sharp and localized lines along the dashed lines in Fig. 3. Further, some protrusions between the lines are observed (with a mutual distance of $2d$), which become more pronounced at negative voltages. These protrusions are assigned to silicon atoms.

According to these experimental findings concerning the chemical composition ($\approx 8\,\%$ carbon), the topo-graphic (mutual atom distances), and electronic properties (chains of vanadium atoms) of the investigated surface as outlined above, a structural model for the reconstructed surface areas is proposed in the following. The top-most unreconstructed $V_3Si(001)$ surface layer is shown in Fig. 4(a), where silicon and vanadium atoms are indicated by small and large spheres, respectively. Two neighboring vanadium lines of the top-most unreconstructed surface layer are proposed to form double rows [Fig. 4(c)]. Every other double row of vanadium moves below the silicon sublattice into the second crystal layer whereas the other vanadium double rows move slightly above the silicon sublattice. The distance between the top double rows is $4d$, matching the distance extracted from STM images. Carbon atoms are attached to the lines on top of some silicon atoms. Dimer lines as well as zigzag lines are formed in this way. The distance between two carbon atoms in a dimer line in this model is $2d$. This distance and also the corresponding distance in the zigzag lines is in agreement with the measurements (compare with the inset in Fig. 2). Figure 4(b) shows an STM image of a reconstructed surface area where carbon and vanadium atoms are depicted by spheres. Silicon atoms denoted A and B in Fig. 4(c) are embedded in different environments regarding the neighbor atoms. They are either neighbored by two carbon atoms and four underlying silicon atoms (position A) or by just four silicon atoms (position B). Only the latter silicon atoms can be observed in the reconstructed surface areas as protrusions between the lines [position B in Fig. 4(b)].

B. Superconducting energy gap

V_3Si is a conventional intermediate-coupling superconductor.[21,62] The DOS of the quasi-particles for intermediate-coupling is described according to Eliashberg.[63] For simplicity, in this work we assume the energy gap to be solely temperature-dependent, $\Delta = \Delta(T)$, such that the quasi-particle DOS can be written as the lifetime-broadened BCS expression for the quasi-particle DOS, ρ_{BCS}, given by[64,65]

$$\rho_{BCS}(E,T) = \rho_N(E)\,\mathrm{Re}\left\{ \frac{|E| - i\Gamma}{\sqrt{(E - i\Gamma)^2 - |\Delta(T)|^2}} \right\},$$

(1)

where $\rho_N(E)$ is the DOS of normal conducting electrons and Γ is a lifetime parameter. We consider a broadening due to the temperature as well as a broadening due to the lock-in amplifier by convoluting ρ_{BCS} with the temperature-broadening function as well as with the instrumental broadening function of the lock-in amplifier.[66,67] We assume the lifetime-broadening to be of the order of $0.1\,\mathrm{meV}$[64] whereas the temperature-broadening is around $2.2\,\mathrm{meV}$ full width at half maximum (FWHM) at $7.3\,\mathrm{K}$.[67] Therefore, for our fits the lifetime parameter is set to a small value such that increasing Γ by a factor 2 does not change our results. Thus only the temperature T and the energy gap Δ are used as fit parameters. The dI/dV spectra close to the Fermi energy are normalized to the differential conductance at $-12\,\mathrm{mV}$ (dI/dV_N), which is well outside the energy gap. The current at $12\,\mathrm{mV}$ was set to values between $0.5\,\mathrm{nA}$ and $1\,\mathrm{nA}$. A typical fit to the data (dots) is shown as a solid line in Fig. 5. Best fits are obtained for temperatures between $7.2\,\mathrm{K}$ and $7.8\,\mathrm{K}$, which are in good agreement with the temperature of the experiment. Our fits yield energy gaps $\Delta = (2.1 \pm 0.2)\,\mathrm{meV}$ within this temperature range. According to BCS theory, this corresponds to a maximal energy gap at $0\,\mathrm{K}$ of $\Delta_0 = (2.15 \pm 0.20)\,\mathrm{meV} = (1.47 \pm 0.14)\,k_B T_c$ with $T_c = 17\,\mathrm{K}$. These results are in reasonable accordance with previous measurements.[33,34,35,36,37,38,39,41] However, comparing our results with most recent measurements[33,41] we find slightly lower gap widths, which may be related to structural changes at the surface due to the carbon-induced reconstruction.

To probe a local effect on T_c we acquired dI/dV spectra at different positions of the reconstructed surface, which are defined in the inset of Fig. 6. Normalized spectra of dI/dV were taken either on atoms of the dimer or zigzag pattern (positions A and C) or between the lines (positions B and D). Differences between dI/dV spectra taken at positions A and C and taken at positions B and D are hardly detectable, so that mainly two different dI/dV curves can be observed, which are shown in Fig. 6. Spectra of dI/dV taken at positions A and C (dots) are symmetric with respect to zero voltage whereas those at positions B and D (crosses) are asymmetric. For small negative sample voltages, the differential conductance is
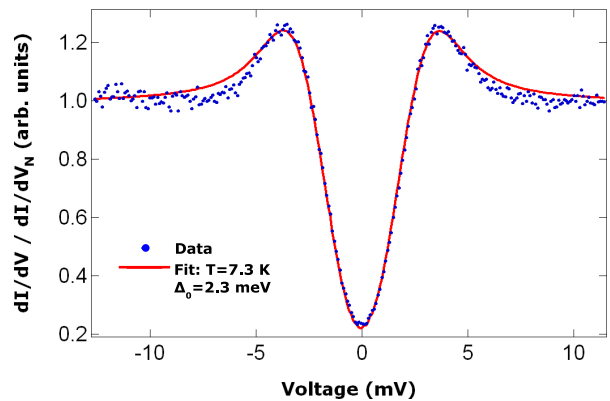

FIG. 5: (Color online) Fit of the BCS quasiparticle DOS (solid line), broadened by the temperature and the modulation voltage used for lock-in amplifier detection of the current response, to normalized dI/dV spectrum (dots). The feedback loop was opened at $12\,\mathrm{mV}$ and $0.5\,\mathrm{nA}$.

higher at positions B and D than at positions A and C. This behavior may be due to the DOS of normal conducting electrons ρ_N, which is different for positions A and C (on the lines) and positions B and D (between the lines). Typically, ρ_N is treated as constant, which leads to a symmetric ρ_{BCS} around the Fermi energy. Since the atomic environment of atoms at different positions of the reconstructed surface areas is different in the present case, it is likely that ρ_N varies locally, too. If ρ_N has asymmetric features within a small energy range around the Fermi energy, the energy gap can be asymmetric. As it can be seen from Eq. (1), the influence of ρ_N can be cancelled by dividing by ρ_N. An angle-resolved photoemission study of $V_3Si(001)$ performed at room temperature revealed the existence of a remarkably sharp peak close to the Fermi level and in the center of the surface Brillouin zone.[32] This contribution to the density of states of normal conducting electrons may give rise to the observed asymmetry of the measured energy gap in spectra of dI/dV. In a first approximation, we divided the asymmetric spectrum by a Lorentzian (maximum at $-5\,\mathrm{meV}$ and FWHM of $29\,\mathrm{meV}$) in order to remove the asymmetry. The result is depicted in Fig. 6 by the solid curve. The asymmetric behavior is nearly compensated and the solid curve fits well with the symmetric dI/dV spectrum.

C. Contact spectroscopy

To perform contact spectroscopy the tip had to be moved controllably into contact with the $V_3Si(001)$ surface. For this purpose we proceeded as reported in Ref. 68 and monitored the conductance ($G = I/V$, I: current, V: voltage) over a range of tip displacements comprising tunneling and contact regimes. Unlike on noble metal surfaces[68,69,70] the contact to $V_3Si(001)$ is
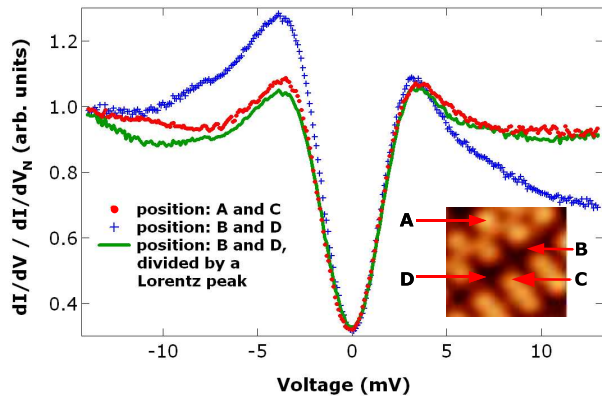
FIG. 6: (Color online) Spectra of dI/dV at constant height close to the Fermi energy at different positions on the reconstructed surface areas (●: position A and C, +: position B and D, positions are denoted in the inset). The feedback loop was opened at $14\,$mV and $0.9\,$nA. Solid line: Spectrum at positions B and D after subtraction of a Lorentzian with a maximum position at $-5\,$meV and FWHM of $29\,$meV.

FIG. 7: Spectra of differential conductance (dI/dV) for different junction conductances. The spectra are normalized to the conductance value at -14 mV (dI/dV_N) and are shifted vertically by $0.2\,$arb. units with respect to each other. The feedback loop was opened at $14\,$mV and $0.7\,\mu$A, $3.5\,\mu$A, $5.0\,\mu$A, and $6.5\,\mu$A. Fits (solid lines), according to Ref. 85, and fit parameters are shown.

not always signaled by a jump of the conductance. We also observed a continuous transition from the tunneling to the contact regime. Contact conductances are defined according to the procedure exposed in Ref. 71. Contact conductances defined in this way scatter between $\approx 1\,\mathrm{G_0}$ and $\approx 3\,\mathrm{G_0}$ where $\mathrm{G_0} = 2e^2/h$ denotes the quantum of conductance (h: Planck's constant). Once the contact regime is reached the tip could be moved further into the surface increasing the conductance to up to $\approx 6\,\mathrm{G_0}$ without destroying the sample surface and tip integrity. From conductance curves acquired in the tunneling regime we inferred the apparent barrier height within a one-dimensional model of the tunneling junction.[72,73,74] The apparent barrier height (Φ_{ap}) was determined by using a tungsten tip and also by using a gold tip. From our contact measurements we obtained $\Phi_{ap}^{W} =(4.60 \pm 0.5)\,$eV and $\Phi_{ap}^{Au} =(4.19 \pm 0.2)\,$eV. In the simplest case, the work function of the sample (denoted Φ^{V_3Si}) is given by $\Phi^{V_3Si} = 2\,\Phi_{ap} - \Phi^{W/Au}$. Taking into account the work functions for polycrystalline specimen of W, $\Phi^{W} = 4.55\,$eV, and Au, $\Phi^{Au} = 5.1\,$eV, from Ref. 75, the work function of V_3Si is $\Phi^{V_3Si} = (3.96 \pm 0.90)\,$eV. Our result is in agreement with previous measurements of the work function of V_3Si, which yield $4.4\,$eV for single-crystalline $V_3Si(001)$[32] and $4.6\,$eV for a polycrystalline sample.[76]

For contact spectroscopy we proceeded as follows. We first acquired a conductance-versus-displacement curve in order to find the contact regime. We then set a junction conductance corresponding to tip-surface contact and performed spectroscopy of dI/dV as previously reported in Refs. 69,77,78. Typical results for various junction conductances are shown in Fig. 7. The dI/dV spectra are normalized to the conductance value at -14 mV and are shifted vertically with respect to each other. The en-
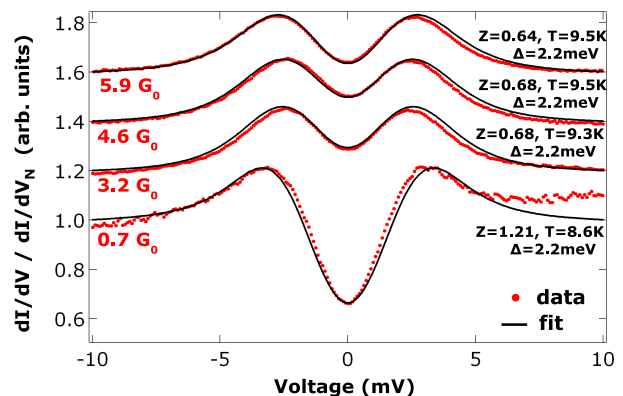
ergy gap in the dI/dV spectra becomes less pronounced at higher conductances of the junction, $i.\,e.$, the indentation of the dI/dV curves between the condensation peaks becomes shallower upon increasing the junction conductance. To model this behavior we first tried to fit the BCS density of states with an increased effective temperature to the data. Several contact experiments have been reported where local heating of the contact junction due to a high current density plays a significant role.[79,80] However, increasing the effective temperature in the BCS density of states, Eq. (1), decreases the condensation peaks, which is not observed in our data.

The apparent change of the superconducting energy gap with increasing junction conductance may be explained by taking Andreev reflections into account.[81,82,83,84] To fit our data, we use a theoretical approach to Andreev reflections at an interface between a normal-metal and a superconductor reported by Blonder $et\,al.$[85] These authors introduced a δ-function potential barrier of strength Z to describe the normal-metal – superconductor interface. For a large barrier strength ($Z = 3.0$) calculated dI/dV spectra agree with dI/dV data acquired in the tunneling regime (Fig. 5). We used the energy gap, Δ, the temperature, T, and the dimensionless barrier strength, Z, as fitting parameters. Fits for the spectra at different conductances are shown in Fig. 7 by solid lines. The quality of the fits is quite remarkable indicating that Andreev reflections play a role in our contact spectroscopy of the $V_3Si(001)$ energy gap.

IV. SUMMARY

STM of $V_3Si(001)$ reveals a surface reconstruction, which is most likely induced by carbon. Based on atom-

ically resolved STM images and on the chemical composition of the surface as monitored by AES we suggest a structural model of this reconstruction. Spatially resolved spectroscopy revealed that the width of the energy gap does not depend on the surface site, while the symmetry of the gap is affected depending on the local environment. The spectroscopic signature of the energy gap changes in the contact regime. These modifications are compatible with Andreev reflections in the point contact between a normal metal tip and a superconductor.

* Electronic address: hauptman@physik.uni-kiel.de
[1] B. T. Matthias, H. Suhl, and E. Corenzwit, Phys. Rev. Lett. **1**, 92 (1958).
[2] A. A. Abrikosov and L. P. Gorkov, Sov. Phys. JETP **12**, 1243 (1960).
[3] M. A. Woolf and F. Reif, Phys. Rev. **137**, A557 (1965).
[4] J. Zittartz, A. Bringer, and E. Müller-Hartmann, Solid State Commun. **10**, 513 (1972).
[5] A. Yazdani, B. A. Jones, C. P. Lutz, M. F. Crommie, and D. M. Eigler, Science **275**, 1767 (1997).
[6] P. W. Anderson, J. Phys. Chem. Solids **11**, 26 (1959).
[7] J. R. Thompson, D. K. Christen, S. T. Sekula, B. C. Sales, and L. A. Boatner, Phys. Rev. B **36**, 836 (1987).
[8] E. W. Hudson, K. M. Lang, V. Madhavan, S. H. Pan, H. Eisaki, S. Uchida, and J. C. Davis, Nature **411**, 920 (2001).
[9] S. Uchida, Physica C **357**, 25 (2001).
[10] S. H. Pan, E. W. Hudson, K. M. Lang, H. Eisaki, S. Uchida, and J. C. Davis, Nature **403**, 746 (2003).
[11] E. Scheer, N. Agraït, J. C. Cuevas, A. Levy Yeyati, B. Ludoph, A. Martín-Rodero, G. Rubio Bollinger, J. M. van Ruitenbeek, and C. Urbina, Nature **394**, 154 (1998).
[12] J. C. Cuevas, A. Levy Yeyati, A. Martín-Rodero, G. R. Bollinger, C. Untiedt, and N. Agraït, Phys. Rev. Lett. **81**, 2990 (1998).
[13] N. van der Post, E. T. Peters, I. K. Yanson, and J. M. van Ruitenbeek, Phys. Rev. Lett. **73**, 2611 (1994).
[14] E. N. Bratus', V. S. Shumeiko, and G. Wendin, Phys. Rev. Lett. **74**, 2110 (1995).
[15] M. Tinkham, *Introduction to Superconductivity*, (McGraw-Hill, Inc., New York, 1996).
[16] Ø. Fischer, M. Kugler, I. Maggio-Aprile, C. Berthold, and C. Renner, Rev. Mod. Phys. **79**, 353 (2007).
[17] C. E. Sosolik, J. A. Stroscio, M. D. Stiles, E. W. Hudson, S. R. Blankenship, A. P. Fein, and R. J. Celotta, Phys. Rev. B **68**, 140503(R)(2003).
[18] N. Bergeal, Y. Noat, T. Cren, Th. Proslier, V. Dubost, F. Debontridder, A. Zimmers, D. Roditchev, W. Sacks, and J. Marcus, Phys. Rev. B **78**, 140507(R) (2008).
[19] J. Muller, Rep. Prog. Phys. **43**, 641 (1980).
[20] G. F. Hardy and J. K. Hulm, Phys. Rev. **5**, 1004 (1954).
[21] S. V. Vonsovsky, Yu. A. Izyumov, and E. Z. Kurmaev, *Superconductivity of Transition Metals*, (Springer-Verlag, Berlin, 1982).
[22] A. M. Clogston, A. C. Gossard, V. Jaccarino, and Y. Yafet, Phys. Rev. Lett. **9**, 262 (1962).
[23] F. J. Morin and J. P. Maita, Phys. Rev. **129**, 1115 (1963).
[24] H. J. Williams and R. C. Sherwood, Bull. Am. Phys. Soc. **5**, 430 (1960).
[25] C. Paduania and C. A. Kuhnen, Eur. Phys. J. B **66**, 353 (2008).
[26] L. R. Testardi, Rev. Mod. Phys. **47**, 637 (1975).
[27] M. Yethiraj, D. K. Christen, D. McK. Paul, P. Miranovic, and J. R. Thompson, Phys. Rev. Lett. **82**, 5112 (1999).
[28] V. G. Kogan, P. Miranovic, Lj. Dobrosavljevic-Grujic, W. E. Pickett, and D. K. Christen, Phys. Rev. Lett. **79**, 741 (1997).
[29] J. E. Sonier, F. D. Callaghan, R. I. Miller, E. Boaknin, L. Taillefer, R. F. Kiefl, J. H. Brewer, K. F. Poon, and J. D. Brewer, Phys. Rev. Lett. **93**, 017002 (2004).
[30] M. Yethiraj, D. K. Christen, A. A. Gapud, D. McK.Paul, S. J. Crowe, C. D. Dewhurst, R. Cubitt, L. Porcar, and A. Gurevich, Phys. Rev. B **72**, 060504(R) (2005).
[31] G. Zajac, J. Zak, and S. D. Bader, Phys. Rev. B **27**, 6649 (1983).
[32] M. Aono, F. J. Himpsel, and D. E. Eastman, Solid State Commun. **39**, 225 (1981).
[33] Yu. A. Nefyodov, A. M. Shuvaev, and M. R. Trunin, Europhys. Lett. **72**, 638 (2005).
[34] H. J. Levinstein and J. E. Kunzler, Phys. Lett. **20**, 581 (1966).
[35] J. J. Hauser, D. D. Bacon, and W. H. Haemmerle, Phys. Rev. **151**, 296 (1966).
[36] J. Schumaun and D. Elefant, Phys. Status Solidi B **95**, 91 (1979).
[37] D. F. Moore, R. B. Zubeck, J. M. Rowell, and M. R. Beasley, Phys. Rev. B **20**, 2721 (1979).
[38] W. Bangert, J. Geerk, and P. Schweiss, Phys. Rev. B **31**, 6066 (1985).
[39] D. B. Tanner and A. J. Sievers, Phys. Rev. B **8**, 1978 (1973).
[40] R. Hackl, R. Kaiser, and W. Gläser, Physica C **162-164**, 431 (1989).
[41] E. Reinert, G. Nicolay, S. Hüfner, U. Probst, and E. Bucher, J. Electron Spectrosc. Relat. Phenom. **114-116**, 615 (2001).
[42] H. Suhl, B. T. Matthias, and L. R. Walker, Phys. Rev. Lett. **3**, 552 (1959).
[43] V. Moskalenko, Fiz. Met. Metalloved. **8**, 503 (1959).
[44] J. Bardeen, L. N. Cooper, and J. R. Schrieffer, Phys. Rev. **108**, 1175 (1957).
[45] C. C. Chang, Surf. Sci. **25**, 53 (1971).
[46] L. E. Davis, N. C. MacDonald, P. W. Palmberg, G. E. Riach, and R. E. Weber, *Handbook of Auger Spectroscopy*, (Physical Electronics Industries).
[47] V. Derycke, P. Soukiassian, A. Mayne, G. Dujardin, and J. Gautier, Phys. Rev. Lett. **81**, 5868 (1998).
[48] V. Yu. Aristov, P. Soukiassian, A. Catellani, R. DiFelice, and G. Galli, Phys. Rev. B **69**, 245326 (2004).
[49] A. Tejeda, E. Wimmer, P. Soukiassian, D. Dunham, E. Rotenberg, J. D. Denlinger, and E. G. Michel, Phys. Rev. B **75**, 195315 (2007).
[50] M. Bode, R. Pascal, and R. Wiesendanger, Surf. Sci. **344**, 185 (1995).
[51] A. M. Clogston and V. Jaccarino, Phys. Rev. **121**, 1357

(1961).

[52] M. Wegner, Rev. Mod. Phys. **36**, 175 (1964).

[53] J. Labbé and J. Friedel, J. Phys. Radium **27**, 153 (1966).

[54] L. F. Mattheiss, Phys. Rev. **138**, A112 (1965).

[55] L. F. Mattheiss, Phys. Rev. B **12**, 2161 (1975).

[56] B. M. Klein, L. L. Boyer, D. A. Papaconstantopoulos, and L. F. Mattheiss, Phys. Rev. B **18**, 6411 (1978).

[57] P. K. Lam and M. L. Cohen, Phys. Rev. B **23**, 6371 (1981).

[58] L. F. Mattheiss and W. Weber, Phys. Rev. B **25**, 2248 (1982).

[59] O. Bisi and L. W. Chiao, Phys. Rev. B **25**, 4943 (1982).

[60] G. Panaccione, J. Fujii, I. Vobornik, G. Trimarchi, N. Binggeli, A. Goldoni, R. Larciprete, and G. Rossi, Phys. Rev. B **73**, 035431 (2006).

[61] G. Trimarchi and N. Binggeli, Phys. Stat. Sol. B **243**, 2105 (2006).

[62] C. P. Poole, H. A. Farach, and R. J. Creswick, *Superconductivity*, (Academic Press, New York, 1995).

[63] G. M. Eliashberg, Zh. Eksp. Teor. Fiz. **38**, 966 (1960).

[64] R. C. Dynes, V. Narayanamurti, and J. P. Garno, Phys. Rev. Lett. **41**, 21, 1509 (1978).

[65] A. S. Alexandrov, *Theory of superconductivity - from weak to strong coupling*, (Institute of Physics Publishing, Bristol, 2003)

[66] J. Klein, A. Léger, M. Belin, D. Défourneau, and M. J. L. Sangster, Phys. Rev. B **7**, 2336 (1973).

[67] J. Kröger, L. Limot, H. Jensen, R. Berndt, S. Crampin, and E. Pehlke, Prog. Surf. Sci. **80**, 26 (2005).

[68] L. Limot, J. Kröger, R. Berndt, A. Garcia-Lekue, and W. A. Hofer, Phys. Rev. Lett. **94**, 126102 (2005).

[69] N. Néel, J. Kröger, L. Limot, K. Palotas, W. A. Hofer, and R. Berndt, Phys. Rev. Lett. **98**, 016801 (2007).

[70] J. Kröger, H. Jensen, and R. Berndt, New J. Phys. **9**, 153 (2007).

[71] J. Kröger, N. Néel, and L. Limot, J. Phys.: Condens. Matter **20**, 223001 (2008).

[72] J. G. Simmons, J. Appl. Phys. **34**, 1793 (1963).

[73] N. D. Lang, Phys. Rev. B **37**, 10395 (1988).

[74] L. Olesen, M. Brandbyge, M. R. Sørensen, K. W. Jacobsen, E. Lægsgaard, I. Stensgaard, and F. Besenbacher, Phys. Rev. Lett. **76**, 1485 (1996).

[75] H. B. Michaelson, J. Appl. Phys. **48**, 4729 (1977).

[76] F. Heiniger and L. Walldén, Phys. Status Solidi **5**, 82 (1971).

[77] N. Néel, J. Kröger, L. Limot, and R. Berndt, Nano Lett. **8**, 1291 (2008).

[78] N. Néel, J. Kröger, R. Berndt, and E. Pehlke, Phys. Rev. B **78**, 233402 (2008).

[79] N. Néel, J. Kröger, L. Limot, T. Frederiksen, M. Brandbyge, and R. Berndt, Phys. Rev. Lett. **98**, 065502 (2007).

[80] G. Schulze, K. J. Franke, A. Gagliardi, G. Romano, C. S. Lin, A. L. Rosa, T. A. Niehaus, Th. Frauenheim, A. Di Carlo, A. Pecchia, and J. I. Pascual, Phys. Rev. Lett. **100**, 136801 (2008).

[81] P. A. M. Benistant, H. van Kempen, and P. Wyder, Phys. Rev. Lett. **51**, 817 (1983).

[82] R. J. Soulen Jr., J. M. Byers, M. S. Osofysky, B. Nadgorny, T. Ambrose, S. F. Cheng, P. R. Broussard, C. T. Tanaka, J. Nowak, J. S. Moodera, A. Barry, and J. M. D. Coey, Science **282**, 85 (1998).

[83] G. J. Strijkers, Y. Ji, F. Y. Yang, C. L. Chien, and J. M. Byers, Phys. Rev. B **63**, 104510 (2001).

[84] A. F. Andreev, Zh. Eksp. Teor. Fiz. **46**, 1823 (1964).

[85] G. E. Blonder, M. Tinkham, and T. M. Klapwijk, Phys. Rev. B **25**, 4515 (1982).

[86] Yu. V. Sharvin, Zh. Eksp. Teor. Fiz. **48**, 984 (1965).